

Extragalactic background light absorption signal in the TeV γ -ray spectra of blazars.

V. V. Vassiliev¹

*Whipple Observatory, Harvard-Smithsonian CfA, P.O. Box 97, Amado, AZ
85645, USA*

Abstract

Recent observations of the TeV γ -ray spectra of the two closest active galactic nuclei (AGNs), Markarian 501 (Mrk 501) and Markarian 421 (Mrk 421), by the Whipple and HEGRA collaborations have stimulated efforts to estimate or limit the spectral energy density (SED) of extragalactic background light (EBL) which causes attenuation of TeV photons via pair-production when they travel cosmological distances. In spite of the lack of any distinct cutoff-like feature in the spectra of Mrk 501 and Mrk 421 (in the interval 0.26 – 10 TeV) which could clearly indicate the presence of such a photon absorption mechanism, we demonstrate that strong EBL attenuation signal (survival probability of 10 TeV photon $< 10^{-2}$) may still be present in the spectra of these AGNs. This attenuation could escape detection due to ambiguity of spectra interpretation between intrinsic properties of the sources and absorption by EBL. By estimating the minimal and maximal opacity of the universe to TeV γ -ray photons, we calculate the visibility range for current and future γ -ray observatories, and show that the Whipple γ -ray telescope should be able to detect (in 10 hours at a 5σ confidence level) a BL Lac object with properties similar to Mrk 501 during its peak activity located at distances up to $z = 0.12$. The proposed atmospheric Cherenkov telescope array VERITAS should be able to see such an object at least as far as $z = 0.3$. Finally, we show that the proposed experiments, VERITAS, HESS, and MAGIC, may even be able to actually *measure* the EBL SED because their observations extend to the critical 75 – 150 GeV regime. In this transition region a distinct “knee-like” feature should exist in the spectra of blazars, which is invariant with respect to their intrinsic properties. The change of the spectral index and flux amplitude across this knee, if observed for several blazars, will provide missing pieces of information needed to measure EBL in the wavelength range 0.1 – 30 μm .

Key words: Gamma rays; Background radiation;
Individual (Markarian 501, Markarian 421)
PACS: 98.70.Vc; 98.70.Rz

¹ Corresponding author: vvassiliev@cfa.harvard.edu

1 Introduction

It was noted first by Gould and Schröder (1) in the late sixties “that observations of cosmic photons in the region 10^{12} to 10^{13} eV would be of great value, since in this region absorption due to the cosmic optical photons is important. In fact, this may provide a means of determination of the optical photon density and of testing cosmological models.” Although the authors pointed out that quasars may be the potential sources for such observations, and the ground-based Cherenkov technique could be the means of study, the real possibility to utilize this idea came one quarter of a century later with the discovery of TeV extragalactic γ -ray sources by the Whipple collaboration. These are low-redshift BL Lac objects Markarian 421 ($z = 0.031$) (2), Markarian 501 ($z = 0.033$) (3), and 1ES2344+514 ($z = 0.044$) (4). The detection of a more distant X-ray BL Lac object, PKS 2155-304 ($z = 0.117$), has been recently reported by the Durham group (5).

Interest in the absorption of extragalactic γ -radiation in recent years has been supported by two reasons: understanding the observational range for extragalactic sources of the very high energy photons (above ~ 1 TeV) and estimating the density of the EBL photons of rather low energy (below ~ 1 eV). The first motivation is of great importance for future γ -ray experiments, such as VERITAS (6), HESS (7), and MAGIC (8), and for testing of blazar emission models (9; 10; 11; 12). The second attracts great theoretical attention, since EBL in the energy range $\sim 10^{-2} - 10$ eV contains a wealth of information on the early history of the universe providing integral constraints on galaxy and star formation, the initial distribution of stellar masses, metal and dust production, and the rate of re-processing of starlight to infrared wavelengths by the dust (13; 14). It is also possible that a significant fraction of the EBL is contributed by brown dwarfs, accreting black holes in active galactic nuclei (AGNs), and the decay of relic particles (15; 16). Because the EBL contains a significant fraction of all energy released since the recombination epoch, its determination may set a limit on the energetic balance of the universe and constrain particular energy sources (13).

Diffuse Infrared Background Experiment (*DIRBE*) and Far Infrared Absolute Spectrometer (*FIRAS*) instrument on board the Cosmic Background Explorer (*COBE*) spacecraft (17) have been used to complete an effort to directly detect an isotropic EBL in ten photometric bands from 1.25 to 240 μm (18), and 125 – 2000 μm wavelength interval (19). The detection of the EBL for wavelengths shorter than 140 μm have been greatly impaired by the presence of strong backgrounds from interplanetary dust scattering and emission, stars and galactic foregrounds, and from interstellar dust emission. Removing these various contaminating radiations to detect a directionally isotropic signal, which is presumably a unique feature of EBL, is a difficult task (20; 21).

The *COBE* collaboration reported a detection of the EBL signal at 140 and 240 μm , but established only upper limits in the region 1.25 – 100 μm (18), the most important interval for attenuation of extragalactic TeV γ -rays. Thus, observation of TeV and sub-TeV extragalactic sources is currently the only relatively direct method which may provide new insight on the distribution of EBL in this wavelength range.

There are two alternatives which can be used to constrain the EBL spectral energy density from γ -ray observations. First is to model EBL spectra based on the knowledge of galaxy and star evolution, and use it to find the optical depth $\tau(E, z)$ and survival probability $\exp(-\tau(E, z))$ for γ -rays of energy E traveling from a source at redshift z . The spectrum of a particular source can be interpreted then as modified by energy-dependent EBL attenuation. Such predictions of the opacity of the universe to $\sim\text{TeV}$ photons have been reported in (22; 14; 23; 24). Many more models have been suggested which derive the EBL SED based on observational constraints and theoretical assumptions (for a summary and references see (13)). These EBL predictions, which can be easily converted into a γ -ray optical depth, are roughly classified in two categories: backward and forward evolution models. The former models adopt current observations of spectra of galaxies as a function of luminosity and translate them backward in time using data on the redshift evolution of galaxy emissivity. An example of such empirically based calculations is given by Malkan & Stecker (25). The latter models tend to simulate the evolution of galactic systems forward in time assuming initial parameters which do not conflict with current observational data, e.g. (26; 27). A clear advantage of these models is the possibility to test various scenarios, and, if the EBL is observed to have certain features in a spectrum, it may be possible to deduce information about cosmology, galaxy and star formation, as well as absorption and radiation of the light by dust. Both backward and forward evolution models do not guarantee, however, that all potential contributors to the EBL are accounted for and therefore more direct constraints on EBL spectral energy density are desirable. Such an alternative, which attempts to unfold the EBL SED from spectral measurements of extragalactic sources, has been explored recently by Stanev & Franceschini, and Biller et al. (24; 28). In this paper we follow an analogous strategy to establish limits on EBL from the spectral measurements of two AGNs, Mrk 421 and Mrk 501, and define applicability conditions of such an approach.

The interpretation of the EBL limits derived from TeV γ -ray measurements is difficult because the EBL absorption cannot be completely isolated from the properties of the source. Although, this problem may be overcome in the future when more TeV and sub-TeV sources are discovered and the physics of the γ -ray emission from blazars is better understood, at present, this feature of the method remains a major source of uncertainty. The credibility of these derivations of the EBL limits from TeV AGN γ -ray measurements is still not

accepted (18; 13). The claim of the first measurement of the EBL by de Jager et al. (29) derived from an apparent “cutoff” in the spectra of Mrk 421 at 4.1 TeV (30) has not been confirmed. More recent measurements of the spectra of Mrk 421 and Mrk 501 (31; 32; 33) are of much better quality but the interpretation is not unambiguous. The Whipple group (32) find curvature in the spectrum of Mrk 501 but conclude that the spectrum of Mrk 421 is consistent with a simple power law up to 10 TeV. The curvature in the spectrum of Mrk 501 is confirmed by the HEGRA group with high precision (33). Because of the apparent differences in the curvature in the spectra of the two AGNs (significant only at the ~ 2 sigma level), Krennrich et al. (31) suggest there is no evidence for EBL absorption. Stecker has recently revised an earlier prediction (23) and now suggests that the new spectrum of the flaring Mrk 501 shows EBL absorption and agrees with one of his EBL models (34). The recent investigation by Stanev & Franceschini of the Mrk 501 spectrum (24) has indicated upper limits on the EBL which almost come into conflict with observational evaluations based on deep surveys of extragalactic sources. These authors conclude that “if spectra at TeV energies for extragalactic γ -ray sources like this for Mrk 501 are confirmed with improved statistics, we may be forced to conclude that the process of $\gamma - \gamma$ interaction in the intergalactic space is more complex than expected and that the average intergalactic magnetic field is extremely weak ($B < 10^{-11}$ G).”

In this paper we strive to reconcile these differing interpretations, we attempt to limit the scope of the potential constraints which γ -ray observations may set on the SED of EBL, and we try to confirm some of the earlier results derived from TeV γ -ray measurements. The structure of the paper is as following. The next section, §2, is a summary of the direct EBL experimental detections, upper and low limits. These are important for unfolding SED of EBL from the spectra of blazars because they can be used to normalize the EBL contribution to γ -ray absorption and establish upper and low limits on TeV γ -ray survival probability. Then, in section §3, we consider details of the pair production process, which absorbs high energy photons, and point out several features important for understanding of this fundamental interaction. We also repeat why one would expect a cutoff in the spectra of TeV extragalactic sources caused by the EBL. The next section, §4, analyzes the recently reported spectra of two AGNs which provide data over a wide dynamic range, with high statistical quality. Although no apparent cutoffs have been detected up to 10 TeV, both spectra are consistent with a non zero curvature. In section §5 we demonstrate that although a cutoff feature is possible, it is not necessarily the only indicator of EBL absorption and the lack of a cutoff in the spectra of AGNs does not automatically mean low density of EBL. Such an alternative is explored in detail in this section, and we derive a SED of EBL which eludes detection due to ambiguity in the interpretation of spectral measurements. Then we determine upper and low limits of this EBL component. In section §6, we use these data to predict maximal and minimal attenuation in the spec-

tra of a “Mrk 501-like” blazar at high redshift if such a hypothetical object demonstrates a peak of activity, and compare its flux with the sensitivities of the existing Whipple (35) and proposed VERITAS (6) γ -ray observatories. The last section, §7, is devoted to a discussion.

2 Summary of direct EBL detections, upper and low limits

Fig. 1 depicts the current observational results on the EBL from UV to far-infrared wavelengths. The range from $1.25 \mu\text{m}$ to $240 \mu\text{m}$ is covered by DIRBE results obtained after a complex background subtraction (18). Detections are found at $140 \mu\text{m}$ and $240 \mu\text{m}$. Upper limits are reported for the other bands where foreground emission from the galaxy and interplanetary dust did not allow estimation of the EBL SED. A tentative detection has also been reported at $3.5 \mu\text{m}$ (36), derived with the use of the DIRBE upper limit and a lower limit from ground-based K-band galaxy counts (37). The latter, shown with the filled star in Fig. 1, was assumed to be a detection in this analysis. The upper limits in UV and optical are derived from all-sky-photometry measurements (38; 39; 40; 41). For a more extended review of earlier results in this energy range see (42). Dwek et al. (13) also indicate recent detections in this wavelength range by Bernstein et al. (not shown).

The lower limits obtained from galaxy counts have been derived from IRAS data (43) for $25, 60, 100 \mu\text{m}$. The two data points at 6.7 and $15 \mu\text{m}$ are deduced from ISO data (44) as reported in (24). Pozzetti et al. published ground-based measurements in K-band (45), and derived recently lower limits from the Hubble Deep Field (HDF) observations (46) covering the range $0.36 - 0.81 \mu\text{m}$. The ground-based UV lower limit at $0.2 \mu\text{m}$ is reported by Armand et al. (47). The solid line in Fig. 1 indicates a FIRAS detection of the extragalactic far-infrared background (19) in the range $125 - 2000 \mu\text{m}$. The cosmic microwave background dominates EBL for wavelengths above $\sim 400 \mu\text{m}$.

The dotted line in Fig. 1 shows an example EBL prediction modeled by Primack et al. (14) for a cold dark matter cosmology with non-zero cosmological constant and Salpeter stellar initial mass distribution (48). The main features of the EBL curve, common for the majority of models, are a peak in SED distribution in the range from 0.1 to $10 \mu\text{m}$ formed mainly by starlight accumulated and redshifted through the history of the universe, the so-called stellar EBL component, and a second peak in the range $10 - 1000 \mu\text{m}$ formed by dust re-emission of the previously absorbed starlight, the dust EBL component. The excess of SED prediction in the UV region can be adjusted to observations in this model either by a higher starlight extinction rate by the dust, or by changing the stellar initial mass distribution to the Scalo model (49), which has less mass concentrated in high-mass stars and consequently produces less

UV light. The EBL predictions by the different models vary, and some of them generate less pronounced features, e.g. Malkan & Stecker calculated an EBL with a substantially smaller valley in the 10 μm region (25). This difference is discussed in the last section.

3 The absorption of extragalactic TeV photons

We are interested in the process $\gamma + \gamma \rightarrow e^+ + e^-$, for which the total cross section is

$$\begin{aligned}\sigma(q) &= \frac{3}{8} \sigma_{\text{T}} f(q) \\ f(q) &= q \left[\left(1 + q - \frac{q^2}{2}\right) \ln \frac{1 + \sqrt{1-q}}{1 - \sqrt{1-q}} - (1+q)\sqrt{1-q} \right] \\ q &= \frac{m_e^2}{E\varepsilon} \frac{2}{1 - \cos(\theta)},\end{aligned}\tag{1}$$

where $\sigma_{\text{T}} = 6.67 \times 10^{-25} \text{ cm}^2$ is Thomson scattering cross-section, $m_e = 0.51 \text{ MeV}$ is the mass of the electron, E and ε are the high and low energies of the photons, and θ is the collision angle (see, for example, (50)). The $f(q)$ function, shown in Fig. 2, reaches its maximum at $q = 0.508$, indicating that for a *head on* collision the peak of the interaction cross-section of the γ -ray photon of energy $E \sim 1 \text{ TeV}$ corresponds to pair production with a soft photon of energy $\varepsilon \sim 0.5 \text{ eV}$ ($\lambda \sim 2.5 \mu\text{m}$)

$$\lambda = 2.41 \mu\text{m} \frac{E}{\text{TeV}}.\tag{2}$$

The absorption probability of the high energy photon per unit path length dl by isotropic diffuse radiation with spectral density $dn(\varepsilon)/d\varepsilon$, is given by (see, for example, original calculations by Gould & Schröder (51))

$$\begin{aligned}\frac{d\tau}{dl} &= \frac{3}{8} \sigma_{\text{T}} \int d\varepsilon \int_{\frac{m_e^2}{E\varepsilon}}^1 dx f\left(\frac{m_e^2}{E\varepsilon} \frac{1}{x}\right) 2x \frac{dn(\varepsilon)}{d\varepsilon}, \\ x &= \frac{1 - \cos \theta}{2}.\end{aligned}\tag{3}$$

Eq. (3) can be transformed to the following form

$$\frac{d\tau}{dl} = \frac{3}{8} \sigma_T \int_{\frac{m_e^2}{E}}^{\infty} d\varepsilon \frac{dn(\varepsilon)}{d\varepsilon} F\left(\frac{m_e^2}{E\varepsilon}\right), \quad (4)$$

$$F(q) = 2 q^2 \int_q^1 f(x) x^{-3} dx. \quad (5)$$

Therefore, attenuation of the high energy γ -rays by *isotropic* background photons peaks at the maximum of $F(q)$ ($q = 0.28$), shown in Fig. 2. This gives a characteristic energy of the soft photon $\varepsilon \sim 0.9$ eV for the most effective attenuation of a 1 TeV γ -ray

$$\lambda = 1.33 \mu\text{m} \frac{E}{\text{TeV}}. \quad (6)$$

This energy is almost a factor of two higher than for a head on collision given in Eq. (2). The upper axis in Fig. 1 indicates energies of the γ -ray photons coupled to the wavelengths of the EBL photons via Eq. (6).

The lowest energy of a soft photon important for interaction with a hard photon of energy E is determined by the threshold for pair production in a head on collision

$$\lambda = 4.75 \mu\text{m} \frac{E}{\text{TeV}}. \quad (7)$$

Thus, for example, a 100 TeV γ -ray begins to feel the presence of the CMB, but it is attenuated mostly by the dust EBL component.

The highest energy ε relevant to interactions with extragalactic photons of energy E should be derived from the properties of the function $F(q)$. The asymptotic behavior of this function at small q (large ε)

$$\lim_{\varepsilon \rightarrow \infty} F\left(\frac{m_e^2}{E\varepsilon}\right) \rightarrow 2 \frac{m_e^2}{E\varepsilon} \left(\ln \frac{4E\varepsilon}{m_e^2} - 2 \right) \quad (8)$$

converges very slowly to zero, such that the integral

$$\int_{\frac{m_e^2}{E}}^{\infty} d\varepsilon F\left(\frac{m_e^2}{E\varepsilon}\right) \rightarrow \infty$$

is divergent at the upper limit. This indicates that interaction of a hard photon of energy E extends far below the characteristic wavelength given by Eq. (6),

and suppression of the integral (4) divergence at large ε is due to the behavior of the EBL spectral density $dn(\varepsilon)/d\varepsilon$. It follows then, that the SED of EBL itself defines the characteristic energy of the soft photon and range of the photon's energy important for intergalactic absorption of a γ -ray with energy E .

As an important example we consider a SED of the form

$$\frac{dn(\varepsilon)}{d\varepsilon} = \frac{\alpha}{\text{eV}} \left(\frac{\varepsilon}{\text{eV}} \right)^{-\beta}, \quad (9)$$

and derive the differential absorption probability

$$\begin{aligned} \frac{d\tau}{dl} &= \frac{3}{8} \sigma_{\text{T}} \alpha g(\beta) \left(\frac{E}{\text{TeV}} \right)^{\beta-1}, \\ g(\beta) &= \left(\frac{\text{MeV}}{m_e} \right)^{2(\beta-1)} \int_0^1 q^{\beta-2} F(q) dq. \end{aligned} \quad (10)$$

Depending on the power index β , the main contribution to this integral comes from the different regions q , and, therefore, from different energy ranges of the EBL field. For $\beta = 2.55$ the function $q^{0.55}F(q)$ is shown in Fig. 2. It peaks at $q = 0.41$ and 90% of the contribution to the integral $g(2.55) = 1.47$ is accumulated when q changes from 0.13 to 0.80. Only 5 percent tails are left below and above this interval. Thus, the range of soft photon wavelengths important for attenuation of γ -ray of energy E is

$$0.62\mu\text{m} \frac{E}{\text{TeV}} < \lambda < 3.8\mu\text{m} \frac{E}{\text{TeV}}. \quad (11)$$

The similar limits derived for $\beta = 2.00$, when value of $g(2.00) = 1.25$, are

$$0.37\mu\text{m} \frac{E}{\text{TeV}} < \lambda < 3.6\mu\text{m} \frac{E}{\text{TeV}}. \quad (12)$$

It can be seen that while low energy end of soft photons remains almost the same for these two examples, the high energy end changes by a factor 1.7 extending the range important for attenuation of γ -ray photons to high energies in the case $\beta = 2.00$.

For a γ -ray of energy, E , which travels cosmological distances from a source at redshift z we generalize Eq. (4) following, for instance (52), to obtain the optical depth

$$\tau(E, z) = \frac{1}{n_0 h_0} \int_0^z \sqrt{1+z} dz \int_{\frac{m_e^2}{E(1+z)^2}}^{\infty} d\varepsilon \frac{dn(\varepsilon)}{d\varepsilon} F\left(\frac{m_e^2}{E\varepsilon(1+z)^2}\right), \quad (13)$$

$$\frac{1}{n_0 h_0} = \frac{3}{8} \sigma_T \frac{c}{H_0},$$

where $H_0 = 100 h_0 \text{ km s}^{-1} \text{ Mpc}^{-1}$ is the Hubble constant, $0.5 < h_0 < 0.85$ is the normalized Hubble expansion rate, c is the speed of light, $n_0 = 4.33 \times 10^{-4} \text{ cm}^{-3}$ is the characteristic density, and $dn(\varepsilon)/d\varepsilon$ is the present-day spectral EBL density. It is also assumed that the density parameter of the universe $\Omega = 1$, cosmological constant $\Omega_\Lambda = 0$, and evolutionary considerations of the EBL spectral density are neglected, which is justified for ($z < 0.3$), implying that the EBL has been produced mostly at higher redshifts (53).

The appearance of a cutoff in the spectra of TeV extragalactic sources has been suggested in one of the pioneering works on TeV γ -ray absorption by Stecker, de Jager and Salamon (54) for quasar 3C 279 ($z = 0.54$) and later several predictions (55; 29; 56; 57) for Mrk 421 have been published. If the differential energy spectrum of a source obeys a power-law, characterized by index δ and flux J one would expect to observe a spectrum modified by EBL absorption

$$\frac{dN}{dE} = J E^{-\delta} \exp(-\tau(E, z)). \quad (14)$$

For an EBL spectral density (9) and small z , the optical depth is given by

$$\tau(E, z) = \frac{\alpha g(\beta) z}{n_0 h_0} \left(\frac{E}{\text{TeV}}\right)^{\beta-1} = \left(\frac{E}{E_c}\right)^{\beta-1}, \quad (15)$$

$$E_c = \left(\frac{n_0 h_0}{\alpha g(\beta) z}\right)^{\frac{1}{\beta-1}} \text{ TeV},$$

and the prediction for an observed spectrum of the source is then

$$\frac{dN}{dE} = J E_c^{-\delta} \exp\left(-\delta \ln\left(\frac{E}{E_c}\right) - \left(\frac{E}{E_c}\right)^{\beta-1}\right). \quad (16)$$

If β is large (as in the original paper which claimed possible EBL measurement (29) from TeV γ -ray observations: $\beta = 2.55$, $\delta = 2.1$), a sharp cutoff must exist in the spectrum because the power-law term in the exponent dominates the logarithmic term at energies above E_c . A lack of events in the preliminary spectrum of Mrk 421 in bins above 3.4 TeV and 5.1 TeV was interpreted as such a cutoff providing an estimate of $E_c = 4.1 \text{ TeV}$. Due to a rapid relative

change of the two terms in the exponent, the logarithmic term dominates for energies below $0.73 E_c = 3.0$ TeV leaving almost no trace of the cutoff at lower energies ($< 0.3 E_c$). Although this detection has not been confirmed in later observations (see next sections §4) the approach to place limits on EBL by “non-detection” of the cutoff feature in AGN spectra remains legitimate. If the spectral measurements of the source extend without a cutoff to an energy E_c , the EBL spectral density (9) is constrained by

$$\alpha < n_0 \frac{h_0}{g(\beta)} z \left(\frac{\text{TeV}}{E_c} \right)^{\beta-1}. \quad (17)$$

It is important to note that as E_c changes in observations, both the α limit and the “window” of EBL photons, which did not produce a cutoff feature at E_c , change according to Eqs. (17, 11, 12). Because this limit depends on the EBL SED model, the model itself must be justified by current theoretical considerations in the corresponding wavelength interval. For example, the region $10 - 100 \mu\text{m}$ is believed to be approximated well with a SED of the form (9) with β in the interval $2 - 3$. Such approximation, however, is invalid for the $1 - 10 \mu\text{m}$ wavelength range. Due to the sensitivity of the γ -ray absorption rate to a rather extended interval of EBL photons (properly explained in Eq. (8)), the optical depth $\tau(E, z)$ is not particularly sensitive to small details of the EBL distribution, they are smoothed out by the integration (Eq. 13). On the other hand, the absorption effect on γ -rays may be exponential, at least for some EBL models (Eq. 16); this is the feature which allows one to establish EBL *upper limits* by a non-detection of the cutoff. Recent Mrk 501 observations by the HEGRA collaboration (33) seem to indicate a rapid decline in the spectrum of this AGN above 10 TeV. If the systematics of HEGRA observations in this energy regime are well understood and these measurements are confirmed, an interpretation of this decline in the Mrk 501 spectrum by EBL absorption may constrain the spectral density in the $10 - 70 \mu\text{m}$ range.

4 Mrk 421 and Mrk 501 spectra

Krennrich et al. (32) have recently published the compiled TeV spectral data of two AGNs, Mrk 421 ($z = 0.031$) and Mrk 501 ($z = 0.033$), shown in Fig. 3. The high statistical quality of these measurements and wide energy range, covering $0.26 - 10$ TeV, allowed for the first time detection of curvature in the Mrk 501 spectrum during its high state of activity. This variable blazar shows changes in the TeV γ -ray flux on a time-scale of several hours (58) with no evidence for temporal variability of the spectral shape observed by the Whipple (59) and HEGRA (60) collaborations. The spectrum remains statistically invariant from the absolute flux which may increase up to several

Crab units² during flaring activity (58; 60).

Mrk 421 is also highly variable showing bursts of radiation on a sub-hour time scale (62), with flux variations of up to 10 Crab units (63). The spectrum of this blazar was derived from three data sets with average fluxes of 2.8, 3.3, and 7.4 Crab units. Neither of these sets has revealed any statistical differences in the spectrum shape justifying compilation of the data (64).

Both spectra are rather featureless in the energy range 0.26 – 10 TeV and do not show an apparent cutoff which could be interpreted as an EBL absorption. Both spectra are well described by a flux dependence

$$\frac{dN}{dE} = J \exp\left(-\delta \ln(E/\text{TeV}) - c \ln^2(E/\text{TeV})\right), \quad (18)$$

where δ is a spectral power index, and c is a curvature. The best fit of such a representation of the data is shown in Fig. 3. It can be seen from the figure that the spectra differ; a χ^2 test places the chance probability that they arise from the same parent distribution as 4×10^{-3} (32). The differences in the two spectra must be due to differences in the intrinsic emission spectra since they are at practically the same redshift; however the fraction of curvature that is common to both spectra could be explained by EBL absorption.

The differences can arise from differences in the spectral index, δ ; in the curvature parameter, c , or in a combination of both. The simplest hypothesis is that a spectrum can be fit by a simple power law ($c = 0$) and, as discussed in (32), the spectrum of Mrk 421 is compatible with this hypothesis. The spectrum of Mrk 501 is not. The spectral indices of the two blazars are statistically different. Fig. 4 depicts the chance probability that a certain value of spectral index can be associated with the data on each object. The curvature parameter in these χ^2 estimates has been fit to the best value at a given index. The statistical quality of the data is enough to rule out the hypothesis of equal spectral indices for the two AGN. A similar analysis of the curvature parameter is not definitive. Although the best fits to c for each source are different (Mrk 421 0.12 ± 0.04 ; Mrk 501 0.20 ± 0.03 (32)) it is also possible to fit both spectra with the same curvature parameter, Fig. 5. Some or all of this curvature could arise from EBL absorption. The peak of the probability ($p_{\chi^2} = 0.1$) is at $c = 0.17$ with the chance probability less than 10^{-3} that the curvature parameter exceeds 0.3.

In the Whipple paper (32) the differences in the spectra of two AGNs were interpreted in the context of synchrotron-inverse Compton (SIC) blazar emission model, and it was concluded that the harder spectral index of Mrk 501

² The Crab unit is defined as the γ -ray flux above 300 GeV from the Crab Nebula (61), i.e. $N_\gamma(E > 300 \text{ GeV}) \approx 10^{-6} \text{ m}^{-2}\text{s}^{-1}$.

and its non-zero curvature is not inconsistent with such a model, if X-ray observations of these objects are attributed to synchrotron emission. It was pointed out that the difference in the energy spectra of Mrk 421 and Mrk 501 must be intrinsic to the sources and not due to intergalactic EBL absorption since both AGNs are located at the same distance $z = 0.03$. It is shown in Fig. 5 that a substantial part of the curvature is not ruled out as common for both blazars, and therefore difference in their curvatures is to be considered as tentative only. Moreover, explaining the curvature of Mrk 421 and Mrk 501 as dominated by EBL absorption seems plausible in the context of SIC model because it is easier to understand than the observed spectral shape independence of these blazars relative to their absolute flux during episodes of activity. When the intrinsic spectrum is almost a pure power-law, it remains invariant with respect to both amplitude and energy re-normalization. If a substantial curvature is present in the intrinsic spectrum, the latter invariance is lost, severely constraining models of blazar flaring (see for example (66)). If, however, the curvature of Mrk 501 is mostly due to EBL absorption, which is not inconsistent with observations of Mrk 421, then changes in the intrinsic hardness ratio of the AGN during flaring may be partially masked by this effect.

In the recent submission (67) by the CAT collaboration on the spectral properties of Mrk 501 the Whipple result on spectral index and curvature of this object has also been confirmed (2.24, 0.22). Unlike the Whipple and HEGRA observations, CAT data seem to indicate spectral variability depending on the state of emission. The detected change of hardness ratio is interpreted in the frame of a SIC blazar emission model with synchrotron target photons, and an interpretation of Mrk 501 flaring activity is suggested as being due to injection of a population of energetic electrons and/or an increase in acceleration efficiency. Although the non-detection of spectral changes by the HEGRA and Whipple collaborations is explained by high energy threshold and low statistics respectively, we think that this result needs further confirmation to reliably disentangle the dynamic and static parts of the spectral index and curvature parameters. The latter should presumably provide a better constraint on the EBL absorption effect.

Both the HEGRA and CAT collaborations have detected a signal above 10 TeV in the spectrum of Mrk 501 during its highstate activity (68; 67) in 1997. The spectral measurements performed with the HEGRA stereoscopic system indicated the presence of an exponential cutoff at 6.2 TeV in the power-law spectra of this object. In the region 0.5 – 10 TeV, however, the reported spectrum is consistent with the Whipple result and can be well described by the power-law with a curvature term. The region above 10 TeV does not follow this dependence and shows a substantially more rapid decline in the AGN flux. Although the cutoff feature on its own does not allow a unique interpretation in terms of EBL limits and/or physical processes generating

radiation at the source, it provides nevertheless a set of interesting constraints suggested in (68), among which an increase in the SED of EBL in the region $30 - 70 \mu\text{m}$ is a possibility.

Because the cutoff above 10 TeV in the spectra of AGNs has been observed only for one object and only by one instrument we do not discuss this feature in our paper due to a variety of alternatives in its explanation. Instead, we refer the reader to several recent publications (69; 70; 71). Alternatively, the region of the Mrk 501 spectrum below 10 TeV is well established and confirmed by several groups including Whipple, CAT, HEGRA, the Telescope Array (72), and the Crimean observatory (73). In addition, spectral measurements of another AGN at a similar redshift, Mrk 421, are known in the same energy range and both spectra are well fitted by a power-law with the curvature term. The HEGRA collaboration has reported recently a Mrk 421 spectrum in a low state of its activity (65) during 1997-1998. Likely due to limited photon statistics, no nightly variability has been found in the spectra of this blazar. The time averaged energy spectrum has been found to be very steep with an index of 3.09 ± 0.07 in the energy range $0.5 - 7$ TeV. Although the significance of the difference between Whipple and HEGRA measurements and its impact on flaring spectral variability of this source remain to be understood, in both measurements the time averaged AGN spectrum is consistent with a pure power-law, but an exponential cutoff or curvature term can be equally well fitted to the data. We use Whipple data which spans the same energy interval ($0.26 - 10$ TeV) to conservatively conclude that curvature, c , of the spectra of the two AGNs caused by intergalactic absorption does not exceed 0.3. The curvature of both AGNs may be due to a common cause, if so, its most probable value is ~ 0.17 .

5 EBL unfolding

The detailed investigation of the spectra of two AGNs has not revealed any “sharp” feature. The non-detection of the cutoff, however, does not automatically mean low EBL spectral density and negligible intergalactic absorption of TeV γ -rays. The featureless spectra of blazars, in fact, allows a non-trivial interpretation. The underlying reason for this is that EBL absorption is difficult to separate from the properties of the source. It can be seen from Eq. (16) that if parameter β of the EBL SED is close to 1, the intergalactic absorption does not produce a distinct feature in a source spectrum. We investigate such a possibility in this section. Our strategy will be just opposite to a prediction of optical depth from EBL spectral density. Instead we accept that $\tau(E, z)$ can be approximated by

$$\tau(E, z) = c_0(z) + c_1(z) \ln\left(\frac{E}{\text{TeV}}\right) + c_2(z) \ln^2\left(\frac{E}{\text{TeV}}\right), \quad (19)$$

which is supported by observations in the energy interval (0.26–10) TeV for a small z . One can think of such an approximation as an expansion series of the $\ln(E/\text{TeV})$ variable, when higher orders produce undetectable contributions in a given energy interval for known spectra of blazars. Using this optical depth representation, we unfold the corresponding EBL spectral density.

To simplify our considerations, we assume at the moment that the redshift of the source is very small ($z \ll 1$). Using formula (13) we obtain an integral equation

$$\int_{\frac{m_e^2}{E}}^{\infty} d\varepsilon \frac{dn(\varepsilon)}{d\varepsilon} F\left(\frac{m_e^2}{E\varepsilon}\right) = \frac{n_0 h_0}{z} \tau(E), \quad (20)$$

which can be resolved with the use of a *Mellin* transformation. Omitting this derivation, we give the final result

$$\begin{aligned} \varepsilon \frac{dn(\varepsilon)}{d\varepsilon} &= \frac{n_0 h_0}{z} \int_{\frac{m_e^2}{\varepsilon}}^{\infty} K\left(\frac{m_e^2}{E\varepsilon}\right) \tau(E) \frac{dE}{E}, \\ K(q) &= \frac{1}{2\pi i} \int_{\sigma-i\infty}^{\sigma+i\infty} \frac{q^s ds}{G(s)}, \quad (\sigma > -1), \\ G(s) &= \int_0^1 q^{s-1} F(q) dq. \end{aligned} \quad (21)$$

It can be seen from Eq. (21) that the formal solution $dn(\varepsilon)/d\varepsilon$ which satisfies the optical depth (19) may be represented as

$$\frac{dn(\varepsilon)}{d\varepsilon} = \frac{n_0}{\varepsilon} \left(p_0 - p_1 \ln \frac{\varepsilon}{\varepsilon_0} + p_2 \ln^2 \frac{\varepsilon}{\varepsilon_0} \right) \quad (22)$$

with characteristic energy ε_0 and some constants p_0, p_1, p_2 . We use this form of the EBL spectral density to connect (p_0, p_1, p_2) to (c_0, c_1, c_2) of the optical depth, conducting a direct calculation of integral (13) with arbitrary, but not large redshift ($z < 0.3$) required by an applicability condition of this formula. One can find that

$$c_i = \frac{1}{h_0} \sum_{j=1}^3 p_j t_{ji}(z), \quad (23)$$

where ($i = 1, 2, 3$), and $t_{ji}(z)$ is a redshift dependent matrix. The introduction of a finite redshift, z , does not change our conclusion about the form of the EBL SED (Eq. 22) since the integration order in integral (13) can be changed, and z should be considered then as a parameter. We also use a characteristic energy $\varepsilon_0 = 9.3$ eV ($\lambda = 0.13$ μm) of the isotropic EBL which corresponds to a peak interaction with 100 GeV γ -rays and truncate the SED at this energy. The current TeV and sub-TeV measurements are not very sensitive to the EBL distribution in UV region. The truncation, however, will introduce an error in the optical depth for low energy γ -rays ($E \sim 100$ GeV) and larger z , limiting the applicability of our considerations to the 0.1 – 10 TeV energy regime. We expect, though, that attenuation of 100 GeV γ -rays will be rather small for the range of redshifts investigated here.

Three examples of EBL spectral density described by Eq. (22) are shown in Fig. 7. It is a curious coincidence that these three parametric SED of the EBL can describe well the expected peak in the 0.1 – 10 μm wavelength range of the EBL energy density produced by starlight emitted and redshifted during evolution of the universe. There is no *a priori* reason why the current observational window of TeV astronomy (0.26 – 10 TeV) and requirement that EBL absorption of γ -rays must produce almost power-law modifications to the spectra of extragalactic sources would necessarily require that the EBL SED, which is allowed to have a peak in the wavelength range 0.1 – 10 μm , would coincide with the theoretical expectation based on completely different assumptions. In other words, if the starlight peak were to be shifted to a longer wavelength region by a factor of 5 – 10, any reasonable amount of EBL would necessarily produce a “knee-like” feature in the (0.26 – 10 TeV) spectra of the sub-TeV sources. The starlight EBL peak is located in such a wavelength region that it eludes its apparent detection in the TeV and sub-TeV spectra of blazars due to ambiguity in the interpretation of the spectral measurements.

The direct upper and low limits on the EBL SED (see Fig. 1) restrict a possible choice of parameters p_0 , p_1 , and p_2 . For example, p_0 , which defines the SED of EBL at $\lambda = 0.13$ μm , is likely limited to (0.025 – 0.45) range by Armand et al. (47) 0.2 μm lower and by Bowyer (38) 0.165 μm upper limits. While the exact choice of this parameter affects the optical depth of γ -rays with energies around 100 GeV at large z , it has a rather negligible effect on the attenuation of photons in the 0.3 – 10 TeV energy range. Thus its value is not constrained by current TeV observations of the low redshift sources. With the reservation that we do not predict correctly a small optical depth of ~ 100 GeV photons we fix this parameter somewhat arbitrarily, at 0.025, assuming that EBL attenuation will unlikely be lower than the one we find.

The limitations imposed on the choice of parameters p_1 and p_2 are shown in Fig. 6. The most severe constraints are due to the *DIRBE* upper limit at 3.5 μm and due to lower limits found by Pozzetti et al. (45) for K-band and by Oliver

et al. (44) at $15 \mu\text{m}$. The upper limits in the wavelength range $0.165 - 0.512 \mu\text{m}$ may potentially constrain the p_1 parameter as it is shown. At the same time these limits affect little the value of p_2 which mostly determines the EBL SED at longer wavelengths and absorption of TeV γ -rays. The p_1 parameter may affect the optical depth in the range $0.3 - 1 \text{ TeV}$. However, if survival probability of such photons is close to one, formula (22) may not be well justified and in this case limits on p_1 from the EBL UV region may become invalid. On the other hand, if the opacity of intergalactic media to such γ -rays is large (≥ 1), these limits must be taken into account. Gamma-ray spectral measurements of sources with larger z , such as the recently discovered (5) X-ray BL Lac PKS 2155-304 ($z = 0.117$), may provide important information to resolve this question.

In the case of Mrk 421 and Mrk 501, the matrix $t_{ji}(z)$ which connects the parameters of the EBL SED to parameters of optical depth is

$$t_{ji}(0.032) = \begin{pmatrix} 0.043 & 0.007 & -0.002 \\ 0.080 & 0.041 & 0.003 \\ 0.182 & 0.168 & 0.041 \end{pmatrix}. \quad (24)$$

The elements of the t_{ji} upper triangle are not exactly equal to zero because we truncated the SED of EBL at 9.3 eV , but they are negligible. One can see that curvature in the spectra of these AGNs is driven by the p_2 parameter

$$c_2 = \frac{1}{h_0} 0.041 p_2. \quad (25)$$

Although the upper limit on $c_2 < 0.3$ (see §4) is consistent with the *DIRBE* $3.5 \mu\text{m}$ limit, it provides no additional constraint on $p_2 < 7.3h_0$ for a reasonable range of the normalized Hubble constant ($0.5 < h_0 < 0.85$). The preferred value of $c_2 = 0.17$, if considered to be dominated by EBL absorption, may give an estimate of $p_2 = 4.15h_0$ which is not ruled out for any h_0 from the indicated range.

The change of the AGN spectral index due to EBL absorption

$$c_1 = \frac{1}{h_0} (0.041 p_1 + 0.168 p_2) \quad (26)$$

can range from $0.12/h_0$ to $0.61/h_0$. This is a large interval since it is possible to have ($\sim 0.2 - 1.0$) EBL contribution to the 2.28 spectral index of Mrk 501. Currently we are not able to use this EBL constraint. But once the mechanism of blazar emission is understood and the c_1 contribution is isolated or limited

from the measurements of the AGN spectrum, then Eq. (26) may become an important restriction on the EBL SED.

The total flux from a blazar is another parameter subjected to ambiguous interpretation. We find that the optical depth for a 10 TeV photon is given by

$$\tau(10 \text{ TeV}, z = 0.032) = \frac{1}{h_0}(0.05p_0 + 0.19p_1 + 0.79p_2). \quad (27)$$

The line of equal survival probability of such a photon is shown in Fig. 6. The maximal and the minimal optical depth allowed in the limited region of (p_1, p_2) parameters is reached at $(0., 3.6)$ restricted by the *DIRBE* $3.5 \mu\text{m}$ point, and almost at $(0., 0.7)$ constrained by the Pozzetti et al. (45) $2.2 \mu\text{m}$ measurement. Thus the possible range of optical depths is given by $0.55/h_0 - 2.88/h_0$ or approximately from 1 to 5. In the latter scenario survival probability for such a photon is less than 1%. Fig. 7 shows the EBL SED for these limiting cases of maximal and minimal attenuation of 10 TeV γ -rays. This figure also depicts an example of the SED of EBL which satisfies a tentative EBL detection point reported recently by Dwek & Arendt (36).

Concluding this section we point out an important limitation which concerns our SED solution for EBL given by Eq. (22). This limitation arises from the general problem of “ill-defined” unfolding tasks being very sensitive to small fluctuations in the source function (74), in our case optical depth $\tau(E)$. In principle, the EBL unfolding procedure given by Eq.(21) can be performed for arbitrary $\tau(E)$. We, nevertheless, chose a smooth approximation (19), and obtained a smooth solution (22). If $\tau(E)$ is slightly perturbed, even with statistically small fluctuations, the unfolded SED of EBL may acquire large distortions. This fact, mainly originating from the asymptotic properties of $F(q)$ (see Eq. 8), simply indicates a deficiency in the complete reconstruction of the soft photon density by unfolding of the optical depth. We assume, therefore, that the suggested EBL solution (22) describes a smooth component of the SED. Small perturbations or spectral line features with small amplitudes are possible in the EBL SED as long as they are not detectable in $\tau(E)$ because integration (20) smoothes them out drastically. We also note that if the EBL SED is very small, close to the indicated lowest limit, then formula (22) may also become inapplicable, except in the high energy end, because EBL absorption will be virtually undetectable in the rest of the spectrum.

6 Attenuation of γ -rays by EBL

An uncertainty in the interpretation of AGN spectral measurements when determining an attenuation of the AGN absolute flux and change of its spectral

index because of the EBL intergalactic absorption creates difficulty in the prediction of the visibility range of TeV blazars. We use our maximal and minimal estimates of the EBL SED, found in the previous section, to predict the maximum and the minimum effect of EBL on the observable spectrum of a “Mrk 501-like” blazar at higher redshifts if such a hypothetical object demonstrates a peak of activity. Then we compare its flux with the sensitivities of the existing Whipple (35) and proposed VERITAS (6) γ -ray observatories.

We extrapolate the optical depth $\tau(E, z)$ to higher redshifts by calculating the $t_{ji}(z)$ matrix. Fig. 8 demonstrates the dependence of $c_0(z)$, $c_1(z)$, $c_2(z)$ of the parameterized $\tau(E, z)$ expression (Eq. 19). This figure shows three sets of curves marked 1, 2, and 3. The first set corresponds to a maximal allowed absorption. The third describes the minimal EBL effect based on the already resolved EBL SED from galaxy counts in deep surveys of extragalactic sources. The second set of curves indicates the SED of EBL defined by $(p_1, p_2, p_3) = (0.025, 0., 4.15h_0)$, which is preferable if curvature in the spectra of Mrk 501 and Mrk 421 is dominated by EBL absorption (see §4).

Figure 9 summarizes changes in the spectrum of a “Mrk 501-like” blazar placed at redshifts $z = 0.03, 0.06, \dots, 0.3$. The total flux of this hypothetical AGN is normalized to 10 Crab units, the highest flux ever observed from Mrk 421 (62). The sensitivities of Whipple and VERITAS, marked “W” and “V”, are indicated (6). They are derived for certain cuts on parameters of the atmospheric shower images and correspond to a 5σ detection in 10 hours, or detection of at least five photons in the regime of low background. The sensitivity shown reflects the standard, small zenith angle, observation mode. In the high energy end it can be substantially improved by utilizing the large zenith angle observation technique (32). Two plots “a” and “b” demonstrate the absorption effect for the highest allowable and the lowest resolved EBL. The change of the flux at 100 GeV when z increases is mostly due to a simple distance factor $\sim z^{-2}$. The intergalactic absorption of such γ -rays is small relative to this effect, and our EBL attenuation prediction, which is not reliable in this energy regime, is masked by this factor. For the lowest EBL SED, the distance effect dominates absorption for all shown curves in the energy interval below 2 TeV. In this case, the Whipple telescope should be able to detect such a blazar up to $z \sim 0.18$ during a few days long episode of activity. For the worst-case scenario of intergalactic absorption the Whipple visibility range to such a hypothetical object is limited to $z \sim 0.12$. Thus, it seems that the high variability of blazars is the reason which so far prevents us from detection of such more distant objects, or luminosity of potential TeV blazars is too low to identify them at high redshifts as X-ray emitters. The recently detected X-ray selected BL Lac PKS 2155-304 has been observed to have maximal X-ray output in the range 0.05 – 0.5 keV during active states (75), which is similar to Mrk 421 peaking at a few keV (76). This object showed a similar observed luminosity in X-ray but it is located at $z = 0.117$. The detection of such a

more luminous but more distant BL Lac is certainly not limited to $z < 0.12$ and may extend to higher redshifts.

The new generation of γ -ray observatories, such as VERITAS (6) and HESS (7), should be able to detect “Mrk 501-like” blazars at least up to distances of $z = 0.3$ as shown in Fig. 9a. Due to their much improved ability to survey the sky, the list of identified TeV and sub-TeV emitters will substantially increase. It is interesting to denote then, that these proposed projects may indeed *measure* the EBL because of the extension of their energy range to below 100 GeV. The SED of the EBL is expected to drop very rapidly in the UV above 2 eV making the universe mostly transparent to γ -rays with sub-100 GeV energy. Therefore, in the vicinity of 100 GeV one should see a “knee-like” transition region in the spectra of AGNs where one power-law is replaced with one with a larger spectral index. The position of this feature should be independent of characteristics of blazars, and the accumulated change of spectral index and change of flux amplitude for several objects at known redshifts will define the EBL SED as shown in our calculations. The more accurate EBL unfolding will be possible because measurements in the region 100 GeV and below provide a reference point in the spectra where no EBL absorption effect should be present. The remaining uncertainty related to a particular source intrinsic spectrum, perhaps, will be eliminated when more sources are detected. The visibility range of VERITAS and HESS will not be limited to $z < 0.3$ if TeV and sub-TeV emitters can have a much higher luminosity than Mrk 501.

7 Discussion

The *DIRBE* collaboration has completed analysis of the data on direct measurements of the EBL spectral density and published detections and upper limits (18), which in many wavelength bands substantially exceed limits interesting for the theoretical understanding of the history of the universe. Currently, only TeV γ -ray astronomy can potentially produce any additional constraints in this field. At the moment though, its role as a contributor to our knowledge about EBL was characterized by the *DIRBE* collaboration in a following conclusion (13). “Currently, there is no evidence for any intergalactic absorption in the spectrum of the three TeV sources detected to date. Claimed detections of, or upper limits on the EBL from TeV γ -ray observations should therefore be regarded as preliminary at present.” We acknowledge the fact that some papers seeking to use TeV measurements to detect or limit EBL in some cases may have been based on preliminary judgments of unverified results. However, reliable conclusions derived from TeV γ -ray observations do exist.

The “no cutoff” approach to derive upper limits on EBL discussed in §3 is a

valid method as long as assumptions of the model are justified in the relevant wavelength interval. It might be arguable if the original calculations, presented in the papers (54; 55; 29), have always satisfied this requirement. According to the current paradigm, though, the wavelength regime $10 - 40 \mu\text{m}$ is expected to be dominated by emission from dust, for which EBL spectral density (9) with $\beta = 2.0 - 3.0$ provides an acceptable description. The absence of a cutoff in the spectrum of Mrk 421 at least up to $E_c = 8.8 \text{ TeV}$ ($\beta = 2.55$), or $E_c = 7.0 \text{ TeV}$ ($\beta = 2.00$) translates to the upper limits on the SED of EBL (see Eqs. (17 11, 12) and Fig. 3)

$$\rho_\lambda < 1.6 \times 10^{-3} h_0 \text{ eV cm}^{-3}, \quad 2.0 \mu\text{m} < \lambda < 37 \mu\text{m} \quad (28)$$

$$\rho_\lambda < 1.0 \times 10^{-3} h_0 \left(\frac{\lambda}{10 \mu\text{m}} \right)^{0.55} \text{ eV cm}^{-3}, \quad 4.1 \mu\text{m} < \lambda < 40 \mu\text{m}. \quad (29)$$

Unless the intrinsic spectra of both Mrk 421 and Mrk 501 are exponentially rising to exactly compensate EBL absorption, these limits constrain rather strongly existing EBL models in this wavelength range (see Fig. 10) as they are almost two orders of magnitude lower than the *DIRBE* upper limits at 12 and 25 μm . Kashlinsky et al. (77; 78) derived comparable limits from the search for a fluctuation signal in the *DIRBE* maps which reflects the spatial correlation properties of the galaxies implying that EBL comes from the redshifted light emitted by them. This method relies upon an extended set of assumptions on the evolution of such parameters as the galaxy SED, galaxy luminosity function with redshift, galaxy clustering, dust absorption and re-emission. The effects of intervening dust, among these, are less understood, especially for this wavelength range because the EBL re-processing by dust could have occurred outside of the galaxy which produced it. The limits derived from the “no cutoff” observations of γ -rays, on the other hand, require only the assumption of the EBL SED behavior in a certain wavelength interval and they are applicable *only* to models which satisfy this condition. If one considers the other limits for this wavelength range (shown in Fig. 10) derived from the different assumptions explained below, one can conservatively limit the SED in $10 - 40 \mu\text{m}$ interval to be below $10 \text{ nW m}^{-2} \text{ sr}^{-1}$.

No apparent cutoff due to intergalactic absorption has been observed in the $0.26 - 10 \text{ TeV}$ spectra of the two most-studied AGNs. However, the recently reported spectra of Mrk 421 and Mrk 501 (32) are not inconsistent statistically with a common major contributor to the curvature of the spectra of these blazars, perhaps EBL absorption. This explanation might be preferable because almost pure intrinsic power-law of these sources provides a larger degree of invariance to support the lack of spectral shape variability observed during flaring activity in Mrk 501. This result, however, needs further confirmation.

The fact that no distinct cutoff feature has been observed in the spectra of two blazars allows a non-trivial interpretation of the EBL SED, as shown in this paper. The spectral energy density should have a certain form and coincide with the expected peak in this wavelength region of the SED from starlight emitted and redshifted through the evolution of the universe. It is rather a peculiar coincidence that TeV γ -ray observations currently span an energy range in which the contribution from the EBL absorption to the spectra of extragalactic sources can be masked easily by unknown properties of the source which has a spectrum close to a pure power-law. Extending the energy range to either higher energies or lower ones should identify a cutoff and knee-type features generated by the dust and stellar components of EBL, respectively.

At the moment the upper limit on the EBL SED can be found (see Fig. 10) based on two assumptions. First, we normalize the EBL spectral density at the 3.5 μm *DIRBE* upper limit and, second, we propagate the SED solution to shorter and longer wavelengths requiring that such an EBL SED may generate changes only in the source flux amplitude, spectral index of the power-law, and spectral curvature. These are allowed by observations of Mrk 501 and Mrk 421. The expected rapid decline of the EBL SED in the UV region is also used in these considerations. Our limits in the range 1 – 10 μm are consistent with those previously derived by Biller et al. (28) and by Dwek & Slavin (56). The former work also used the *DIRBE* upper limit for normalization and propagated the allowed SED solution by limiting the range of spectral index changes. Dwek & Slavin were first to study γ -ray absorption by the stellar component of EBL and found high model dependent upper limits in this wavelength range. This is the first work which indirectly proved that a substantial amount of the EBL produced by redshifted starlight may escape detection in TeV γ -ray observations of a source with unknown absolute flux and spectral index.

The limits derived from TeV γ -ray measurements in 1 – 10 μm region seem to be in good agreement with each other except the very low ones given by Stanev & Franceschini (24). These authors also attempted to unfold EBL spectra indirectly from the measurements of Mrk 501, but the absolute flux normalization and power-law spectral index were allowed to vary during the fitting procedure. As we showed in §5, an EBL SED component of the form $\varepsilon(p_0 - p_1 \ln(\varepsilon/\varepsilon_0))$ with arbitrary constants is likely to be undetectable with such a method. Perhaps existence of this hidden invariance was the reason for unstable behavior of the solution which has been found to be crucially dependent on the manner in which power-law fluxes are normalized. If our supposition is valid such a component can be added to the very low upper limits given in this paper until it becomes constrained by one of the experimental points, likely the *DIRBE* 3.5 μm upper limit.

Our low and high estimate of the opacity of the universe to TeV and sub-TeV γ -rays indicate that attenuation should not prevent us from seeing more TeV

sources even with existing γ -ray observational facilities. The future projects, such as VERITAS, HESS, and MAGIC, have a high potential to increase the list of TeV and sub-TeV sources, because they extend their sensitivity range for objects similar to the TeV emitter Mrk 501 up to $z = 0.3$. If there are more luminous objects capable of producing TeV radiation, this redshift will not be a limit.

The TeV and sub-TeV observations have the potential to further contribute in identifying the EBL SED. The HEGRA collaboration has measured recently the Mrk 501 spectrum with very high statistical quality (68). For the first time the energy range of detected γ -rays is extended above 10 TeV up to ~ 20 TeV providing a sensitivity in the $40 - 70 \mu\text{m}$ region of EBL. The rapid decline in the Mrk 501 spectrum found at the highest observed energies suggests several explanations such as intergalactic EBL absorption due to the dust component, intrinsic absorption of γ -rays at the source, or a cutoff in the photon production mechanism (70; 69). Further progress in the analysis of this data can be achieved if spectral and temporal characteristics of the emission in X-ray and TeV regions are found during multiwavelength campaigns or a cutoff feature is identified in the spectrum of Mrk 421 above 10 TeV. In both cases, this will reduce the interpretation ambiguity and perhaps the dust EBL component expected in this wavelength interval will be detected or strongly constrained.

The valley between $10 - 40 \mu\text{m}$ may also become testable. The empirically based calculations of the EBL spectrum by Malkan & Stecker (25) produce a fairly flat EBL SED in this region (see Fig.10). This feature of their EBL model is primarily responsible for a prediction by Stecker (34) of an absorption cutoff above ~ 6 TeV for PKS 2155-304 ($z = 0.117$). It may be that a very large exposure on the source may be necessary to deduce spectrum up to this energy, but if this cutoff is not observed, it will indicate a SED in this region closer to the lines “1-3” shown in Fig. 7 rather than an almost constant EBL SED distribution.

The limits in the wavelength region $\sim 1 - 10 \mu\text{m}$ can be improved if the EBL signal in the spectra of AGNs is isolated, or at least limited, by blazar emission models. Currently, an upper limit on the spectral curvature of Mrk 501 and Mrk 421 does not provide a more strict limit than the *DIRBE* direct upper limit at $3.5 \mu\text{m}$. However, if the most likely curvature, 0.17, in their spectra is due to EBL absorption then the range of possible SEDs is limited by lines marked as “1” and “2” in Fig. 10. These predictions seem to be higher than current EBL theoretical models. This could mean either an additional contribution to EBL from an unidentified source, or that at least part of the blazars’ spectral curvature must be intrinsic to the sources. If the latter is correct, then confirmation of spectral invariance during episodes of activity of blazars may strongly limit flaring mechanisms. Restricting the change of

spectral index, c_1 , due to EBL absorption may impose strict limits on the SED in $\sim 1 - 10 \mu\text{m}$ range. Measurements in the GeV range are available for Mrk 421 (79) which show spectral index 1.57. The spectral index for the best fit in the 0.26 – 10 TeV range with curvature 0.17 gives value 2.48. The 0.91 difference again provide a rather loose constraint on EBL since we already limited this number to be between $0.12/h_0$ and $0.61/h_0$. It is possible to explain such a change in the blazar spectral index purely by γ -ray absorption, again implying a substantial SED of EBL limited by lines “1” and “2” depending on the value of h_0 . There is no argument, however, to support that such change in spectral index could not be intrinsic to the source since these measurements are separated by more than two orders of magnitude in energy. The recent report of a 5.2σ ($E > 0.5$ GeV) detection of Mrk 501 by EGRET (80) estimated the spectral index as 1.3 ± 0.5 again indicating that the largest allowable opacity to TeV photons is possible. It seems that constraints on EBL in the $1 - 10 \mu\text{m}$ wavelength region may come only if the spectrum of a new TeV source will be measured, preferably in TeV, sub-TeV, and GeV regions.

The EBL region $0.1 - 1 \mu\text{m}$ is not constrained well by current sub-TeV observations. This wavelength interval holds crucial information which may finally allow one to determine EBL through the whole range $\sim 0.1 - 10 \mu\text{m}$. VERITAS, HESS and MAGIC should be able to see farther and detect many sources. It is very important that the energy range of these observatories extend to below 100 GeV providing a possibility to measure in one experiment the “turn on” of the effect of sub-TeV γ -ray absorption by EBL. The “knee-like” feature has to exist in the spectra of blazars around 100 GeV, independent of properties of AGNs. The change of the power law through this knee, if observed for several sources, will determine the amount of EBL in this wavelength band. It is very important also that due to the high sensitivity of these experiments the spectra of the closest AGNs Mrk 421 and Mrk 501 will perhaps be measured up to 50 TeV, providing information on the $70 - 140 \mu\text{m}$ EBL window. This will close the last gap in the EBL SED and meet with direct detections by the *FIRAS* and *DIRBE* experiments.

Acknowledgements

I thank F. Krennrich of the Whipple collaboration for providing the spectra of Mrk 421 and Mrk 501, J. Primack and J. Bullock for useful discussion, M. Catanese for valuable discussions and invaluable help, and T. Weekes for thoughtful advice and encouraging this study. This work was supported by grants from the U.S. Department of Energy.

References

- [1] R.P. Gould, & G.P. Schröder, *Phys. Rev.* 155 (1967) 1408.
- [2] M. Punch et al., *Nature* 358 (1992) 477.
- [3] J. Quinn et al., *ApJ* 456 (1996) L83.
- [4] M. Catanese et al., *ApJ* 501 (1998) 616.
- [5] P.M. Chadwick et al., *ApJ*, in press; astro-ph/9810209.
- [6] T.C. Weekes et al., VERITAS proposal (1999).
- [7] F. Aharonian et al., HESS, Letter of Intent (1997).
- [8] J.A. Barrio, The MAGIC telescope, MPI-PhE/98-5 (1998).
- [9] C.D. Dermer, R. Schlickeiser, & A. Mastichiadis, *A&A* 256 (1992) L27.
- [10] L. Maraschi, G. Ghisellini, & A. Celotti, *ApJ* 397 (1992) L5.
- [11] K. Mannheim, *A&A* 269 (1993) 67.
- [12] M. Sikora, M.C. Begelman, & M.J. Rees *ApJ* 421 (1994) 153.
- [13] E. Dwek et al., *ApJ* 508 (1998) 106.
- [14] J.R. Primack et al., *Astropar. Phys.*, in press; astro-ph/9812399.
- [15] J.R. Bond, B.J. Carr, & C.J. Hogan, *ApJ* 306 (1986) 428.
- [16] J.R. Bond, B.J. Carr, & C.J. Hogan, *ApJ* 367 (1991) 420.
- [17] N.W. Boggess et al., *ApJ* 397 (1992) 420.
- [18] M.G. Hauser et al., *ApJ* 508 (1998) 25.
- [19] D.J. Fixsen et al., *ApJ*. 508 (1998) 123.
- [20] T. Kelsall et al., *ApJ* 508 (1998) 44.
- [21] R.G. Arendt et al., *ApJ* 508 (1998) 74.
- [22] D. MacMinn, J.R. Primack, *Space Sci. Rev.* 75 (1996) 413.
- [23] F.W. Stecker, & O.C. de Jager, *A&A* 334 (1998) L85.
- [24] T. Stanev, & A. Franceschini, *ApJ* 494 (1998) L159.
- [25] M.A. Malkan, & F.W. Stecker, *ApJ* 496 (1998) 13.
- [26] R.S. Somerville, & J.R. Primack, *MNRAS*, in press; astro-ph/9802268.
- [27] B. Guiderdoni et al., *Nature* 390 (1997) 257.
- [28] S.D. Biller et al., *Phys. Rev. Lett.* 80 (1998) 2992.
- [29] O.C. de Jager, F.W. Stecker, and M.H. Salamon, *Nature* 369 (1994) 294.
- [30] G. Mohanty et al., *Proc. 23rd ICRC*, 1 (July 19-30, 1993, Calgary) 440.
- [31] F. Krennrich et al., *ApJ* 481 (1997) 758.
- [32] F. Krennrich et al., *ApJ*, 511 (1999) 149.
- [33] A. Konopelko et al., *Astropar. Phys.*, in press; astro-ph/9901093.
- [34] F.W. Stecker, *Astropar. Phys.*, in press; astro-ph/9812286.
- [35] T.C. Weekes et al. *ApJ*, 342 (1989) 370.
- [36] E. Dwek, & R.G. Arendt, *ApJ* 508 (1998) L9.
- [37] J.P. Gardner, in: E. Dwek ed. *Unveiling the Cosmic Infrared Background* (New York: AIP Press 1996) 127.
- [38] S. Bowyer, *ARA&A* 29 (1991) 59.
- [39] M. Maucherat-Joubert et al., *A&A* 88 (1980) 323.
- [40] G.N. Toller, *ApJ* 266 (1983) L79.
- [41] R. R. Dube et al., *ApJ* 232 (1979) 333.
- [42] L.L. Cowie, in: N. Kaiser & A.N. Lasenby eds. *The Post-Recombination*

- Universe* (Kluwer Academic, 1988) 1.
- [43] P.B. Hacking, & B.T. Soifer, ApJ 367 (1991) L49.
 - [44] S.J. Oliver et al., MNRAS 289 (1997) 471.
 - [45] L. Pozzetti et al., MNRAS 281 (1996) 953.
 - [46] L. Pozzetti et al., MNRAS 298 (1998) 1133.
 - [47] C. Armand et al., A&A 284 (1994) 12.
 - [48] E. Salpeter, ApJ 121 (1955) 61.
 - [49] J.M. Scalo, Fund. Cosmic Phys, 11 (1986) 1.
 - [50] W. Heitler, *The Quantum Theory of Radiation* (London: Oxford Press, 1960).
 - [51] R.P. Gould, & G.P. Schröder, Phys. Rev. 155 (1967) 1404.
 - [52] F.W. Stecker, *Cosmic Gamma Rays* (Baltimore: Mono Book Co. 1971).
 - [53] P. Madau, in: S.S. Holt & L.G. Mundy eds. *Star Formation Near and Far*, AIP Symp. Proc. 393 (New York: AIP Press 1996) 481.
 - [54] F.W. Stecker, O.C. de Jager, and M.H. Salamon, ApJ 390 (1992) L42.
 - [55] F.W. Stecker, & O.C. de Jager, ApJ 415 (1993) L71.
 - [56] E. Dwek, & J. Slavin, ApJ 436 (1994) 696.
 - [57] S.D. Biller et al., ApJ 445 (1995) 227.
 - [58] J. Quinn et al., ApJ, in press; astro-ph/9903088.
 - [59] F.W. Samuelson et al. ApJ 501 (1998) L17.
 - [60] F. Aharonian et al., A&A 342 (1999) 69.
 - [61] A.M. Hillas et al., ApJ 503 (1998) 744.
 - [62] J.A. Gaidos et al., Nature 383 (1996) 319.
 - [63] J. Zweerink et al., ApJ 490 (1997) L170.
 - [64] F. Krennrich et al., Invited talk, *Int. Workshop, Taormina, Italy*, in press; astro-ph/9812029.
 - [65] F.A. Aharonian et al., submitted to A&A (1999); astro-ph/9905032.
 - [66] A. Mastichiadis & J.G. Kirk, A&A 320 (1997) 19.
 - [67] A. Djannati-Atai et al., submitted to A&A (1999); astro-ph/9906060.
 - [68] F.A. Aharonian et al., submitted to A&A (1999); astro-ph/9903386.
 - [69] A.K. Konopelko et al., ApJ Letters (1999) in press; astro-ph/9904057.
 - [70] P.S. Coppi and F.A. Aharonian, *Astropar. Phys.*, in press; astro-ph/9903160.
 - [71] P.S. Coppi and F.A. Aharonian, submitted to ApJ (1999); astro-ph/9903159.
 - [72] N. Hayashida98 et al., ApJ 504 (1998) L71.
 - [73] V. Fomin (1999) private communications.
 - [74] A.N. Tikhonov & V.Y. Arsenin, *Solutions of Ill-Posed Problems* (Wiley, 1977).
 - [75] C.M. Urry et al., ApJ 486 (1997) 799.
 - [76] J.H. Buckley et al., in: C. Dermer, M. Strickman, J. Kurfess eds. *Proc. 4th Compton Symposium* (AIP Conf. Proc., 1997) 1381.
 - [77] A. Kashlinsky et al., ApJ 470 (1996) 681.
 - [78] A. Kashlinsky et al., ApJ 473 (1996) L9.
 - [79] R.C. Hartman et al., ApJ (1999) in press.

[80] J. Kataoka et al., ApJ (1999) in press; astro-ph/9811014.

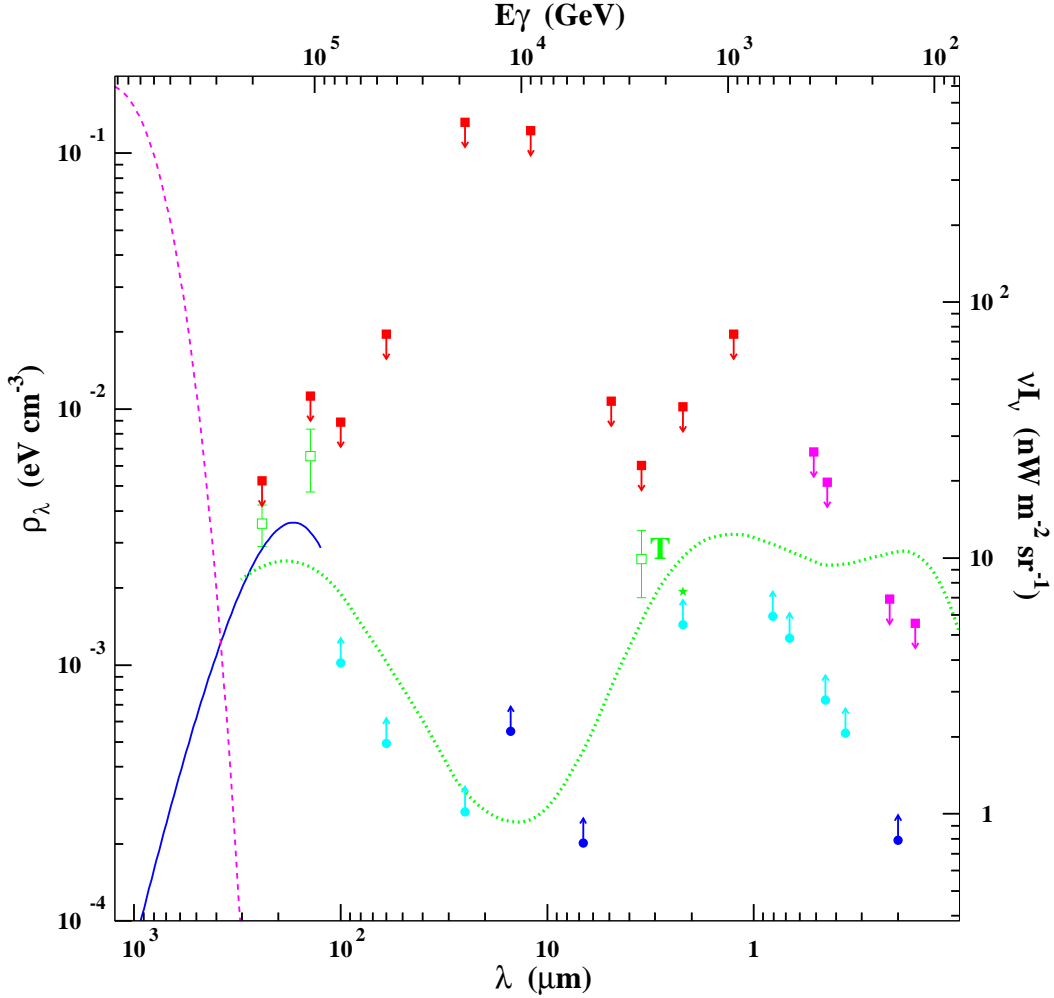


Fig. 1. Filled squares with arrows indicate EBL upper limits (95%CL) determined by various experiments. The wavelength range from 1.25 μm to 240 μm is from the DIRBE experiment (18). Optical and UV bands are by all-sky-photometry observations (38; 39; 40; 41). The open squares at 140 μm and 240 μm are DIRBE detections (shown with 1σ error bars). A tentative detection (36) is indicated by open square marked “T”. The filled circles indicate lower limits (95%CL) obtained from galaxy counts. The range 25 – 100 μm is from IRAS data (43). The 6.7 and 15 μm are from ISO measurements (44). The ground-based measurement at 2.2 μm is reported in (45). The lower limits in the range from 0.36 μm to 0.81 μm are derived from HDF galaxy counts (46). The UV lower limit at 0.2 μm is from (47). The solid line is a FIRAS detection of the far-infrared EBL (19). The dashed line indicates 2.7K CMB radiation. The dotted line is an example of EBL prediction found by Primack et al. for the “LCDM Salpeter” model in (14).

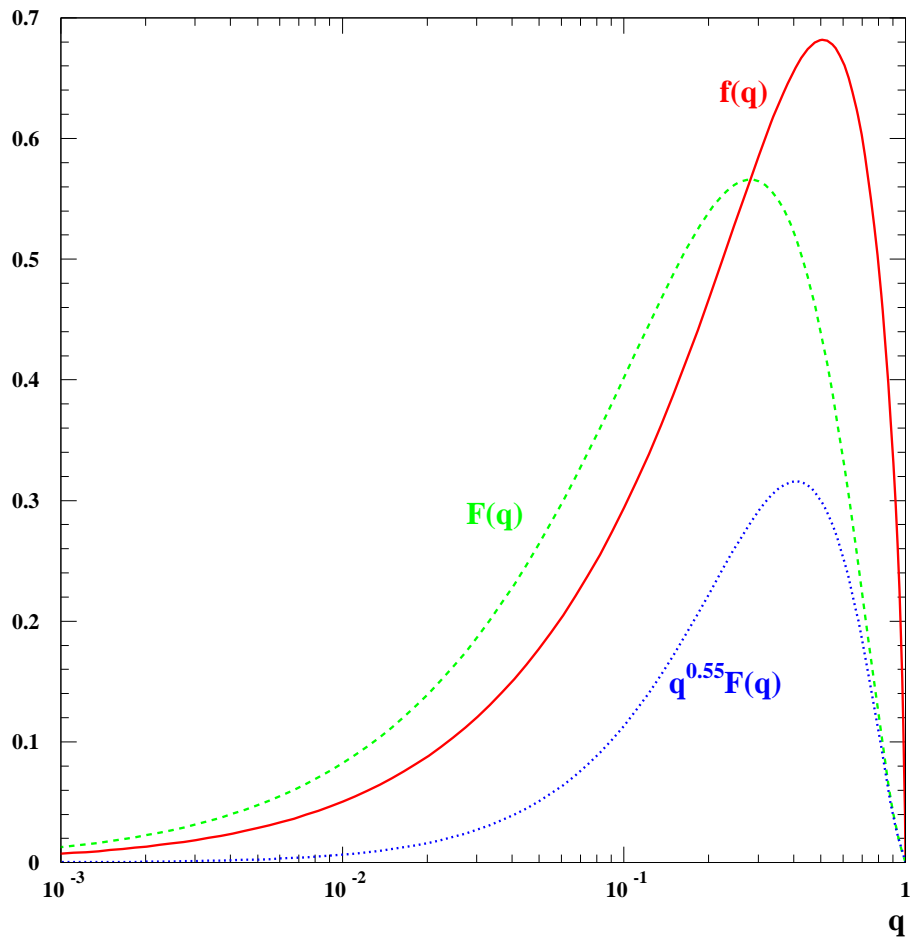


Fig. 2. The behavior of the functions $f(q)$, $F(q)$, and $q^{0.55}F(q)$ which peak at $q = 0.51$, 0.28 , and 0.41 respectively.

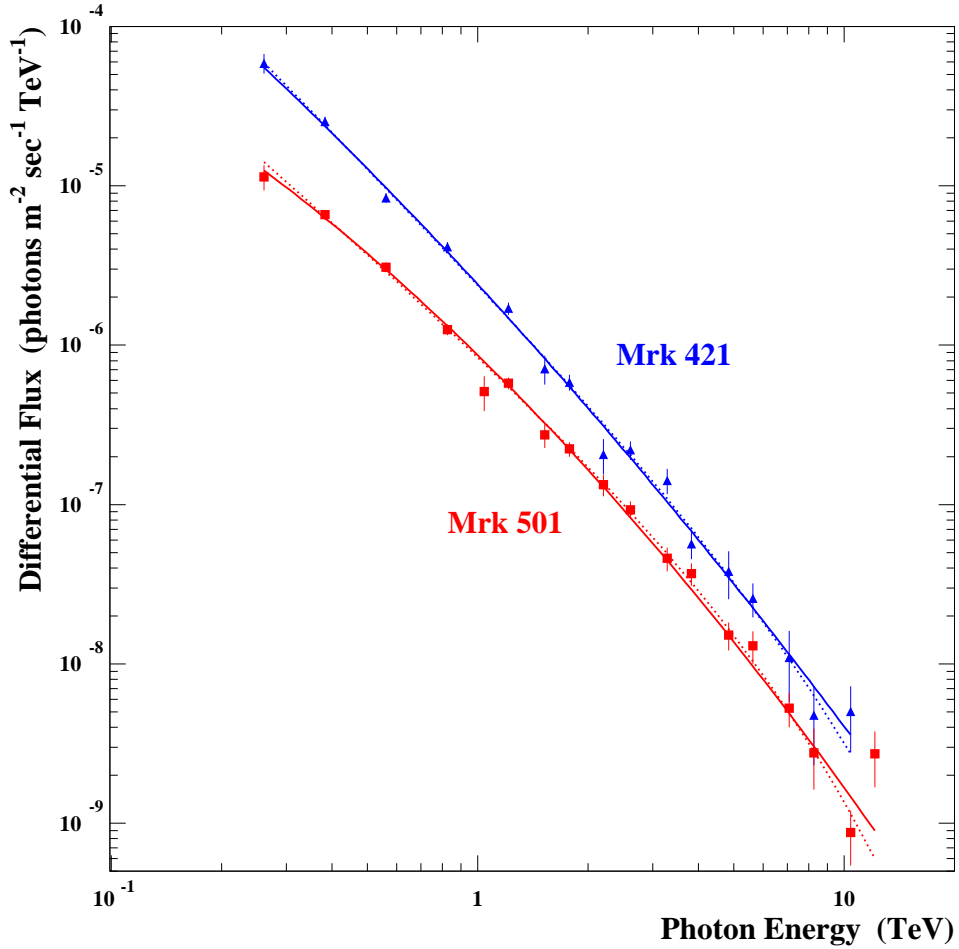


Fig. 3. Spectra of Mrk 421 (filled triangles) and Mrk 501 (filled squares) as reported in (32). The solid lines indicate the best fits of the curved spectra $\sim \exp(-\delta \ln(E/\text{TeV}) - c \ln^2(E/\text{TeV}))$ with parameters (δ, c, p_{χ^2}) for Mrk 421 (2.50, 0.12, 0.14), and Mrk 501 (2.26, 0.20, 0.31). The dotted lines show the best fits of the spectra with exponential cutoff $\sim \exp(-\delta \ln(E/E_c) - E/E_c)$ and parameters $(\delta, E_c, p_{\chi^2})$ for Mrk 421 (2.32, 7.0 TeV, 0.11), and Mrk 501 (1.99, 4.9 TeV, 0.41). Due to variability of the sources the absolute fluxes shown have arbitrary normalization.

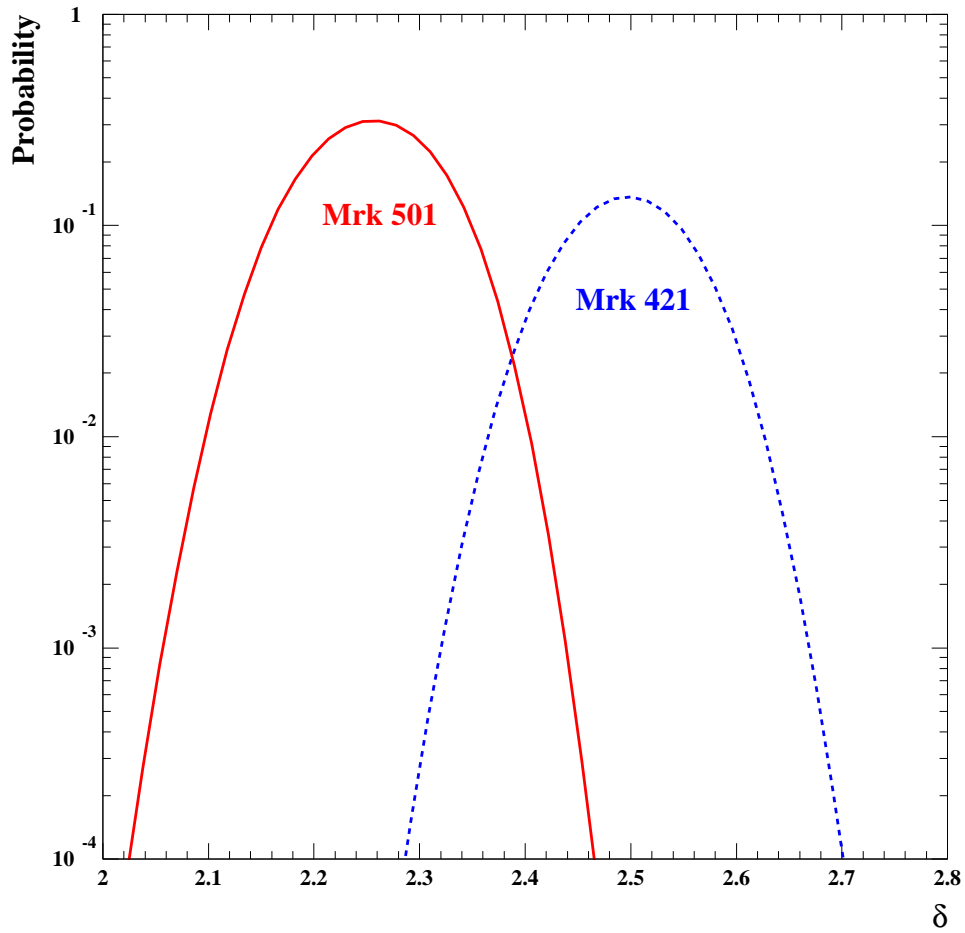


Fig. 4. The chance probability for AGN spectrum to have a certain value of spectral index δ . Mrk 421 peak is at $\delta = 2.50$ with $p_{\chi^2} \leq 10^{-3}$ for $\delta \geq 2.68$, and Mrk 501 peak is at $\delta = 2.26$ with $p_{\chi^2} \leq 10^{-3}$ for $\delta \geq 2.44$.

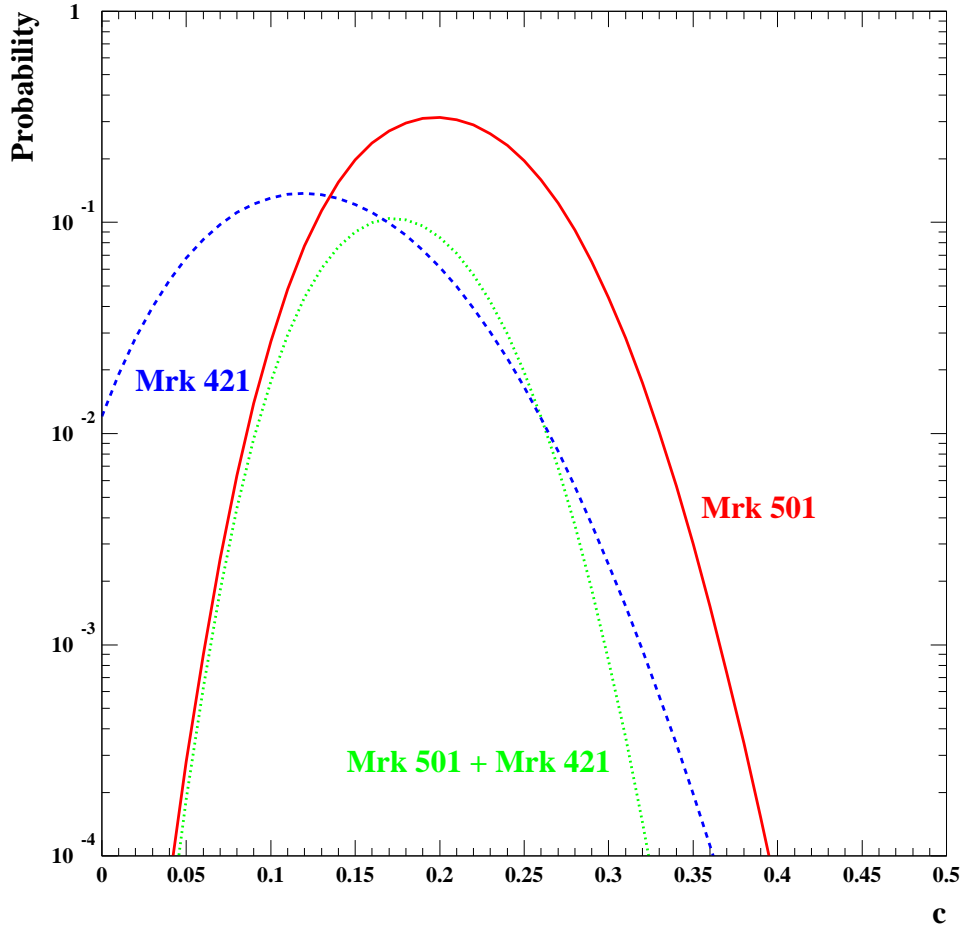


Fig. 5. The chance probability for the AGN spectra to have a certain value of curvature parameter, c . Mrk 421 peak is at $c = 0.12$ with $p_{\chi^2} \leq 10^{-3}$ for $c \geq 0.32$, and Mrk 501 peak is at $c = 0.20$ with $p_{\chi^2} \leq 10^{-3}$ for $c \geq 0.37$. If curvature of the spectra is fixed for both AGNs but the spectral indices are allowed to vary, the combined chance probability for Mrk 421 and Mrk 501 is given by the dotted line. It peaks at $c = 0.17$ with ($p_{\chi^2} = 0.1$), Mrk 421 $\delta = 2.48$, and Mrk 501 $\delta = 2.28$. The chance that $c \geq 0.30$ is less than 10^{-3} .

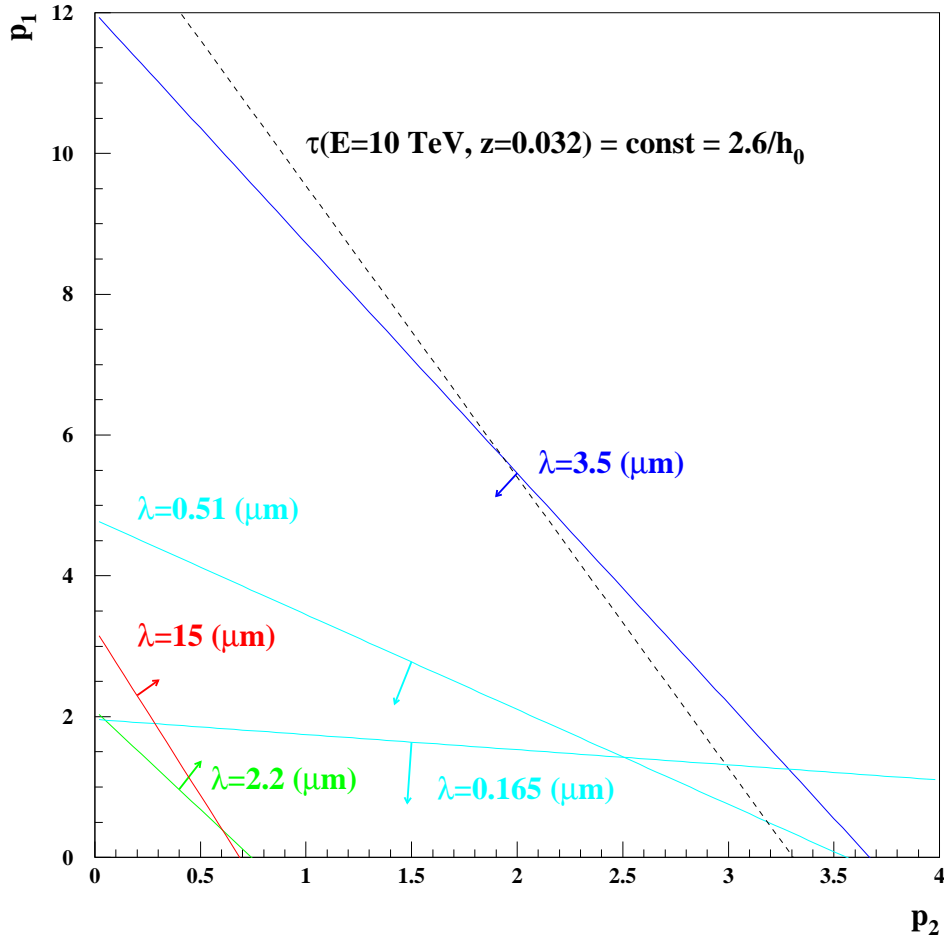


Fig. 6. Constraints on the choice of p_1 and p_2 parameters from existing EBL upper and lower limits. The p_0 parameter is taken to be 0.025. The dashed line indicates constant attenuation of 10 TeV γ -rays at $z = 0.032$. The lines parallel to it would correspond to lower or higher constant optical depth.

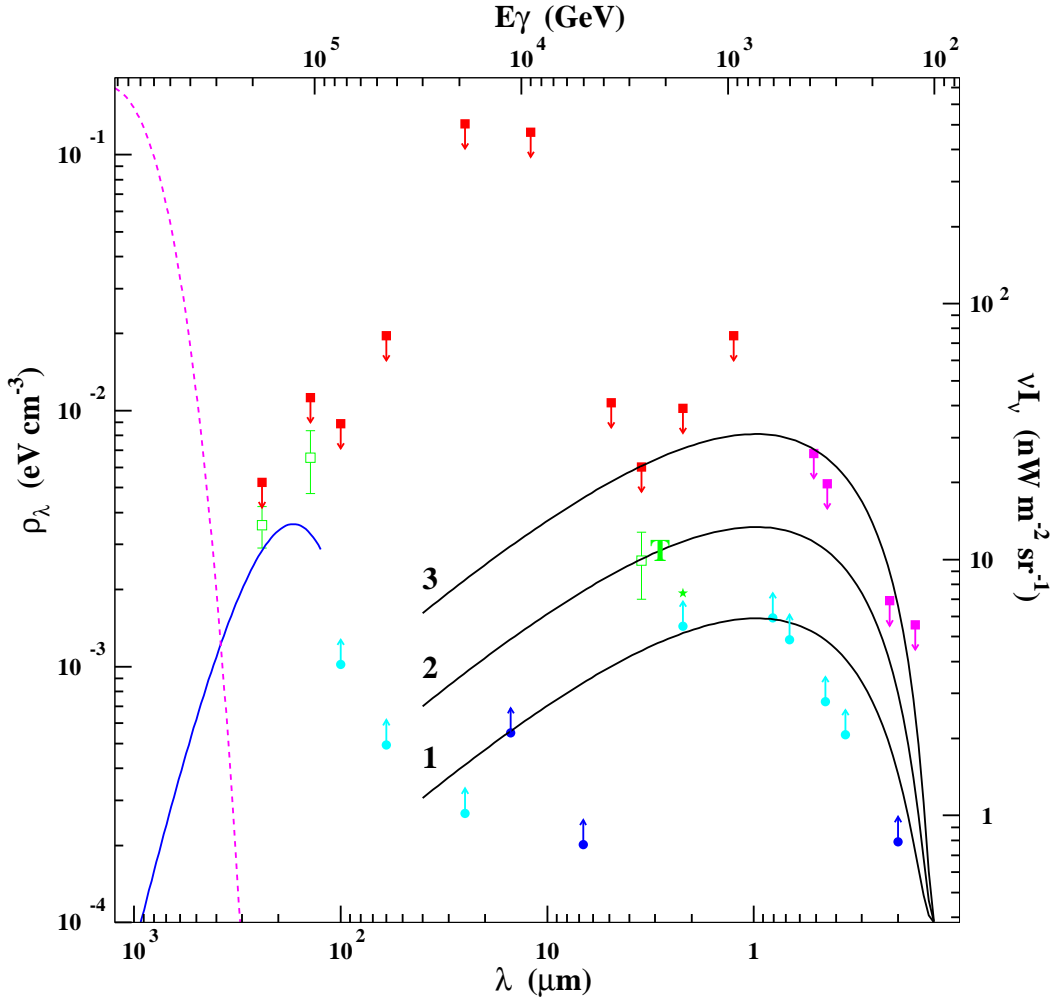


Fig. 7. The examples of SED EBL corresponding to maximal and minimal attenuation of 10 TeV γ -rays consistent with EBL upper and low limits and with observations of the Mrk 421 and Mrk 501 TeV spectra. Line 1 defined by $(p_1, p_2, p_3) = (0.025, 0., 0.7)$ gives minimal optical depth $0.55/h_0$. Line 3, $(0.025, 0., 3.6)$ generates maximal allowable optical depth $2.88/h_0$. Line 2, $(0.025, 0., 1.6)$, shows an example of SED EBL which is consistent with recent tentative EBL detection at $3.5 \mu\text{m}$ (36). This EBL distribution would be responsible for $1.26/h_0$ optical depth.

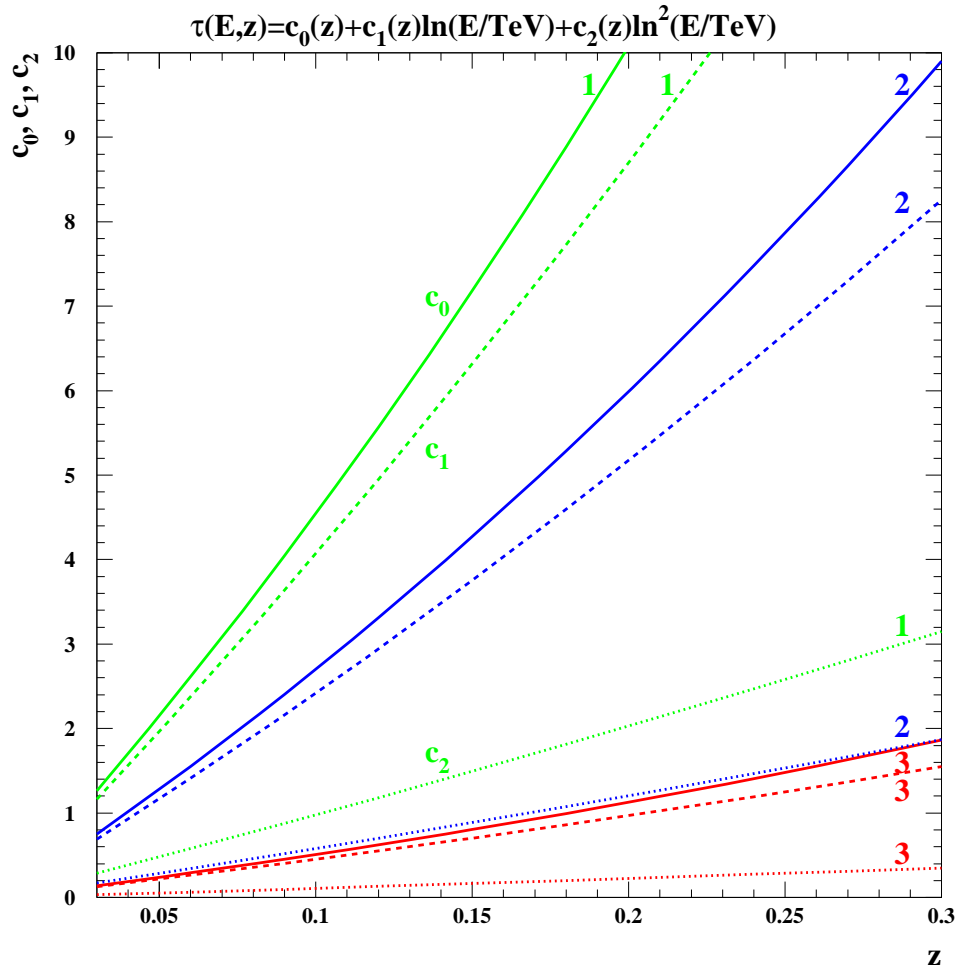


Fig. 8. The dependence of $(c_0(z), c_1(z), c_2(z))$ functions on redshift for the highest allowable EBL absorption effect (marked 1), for the lowest already detected EBL density (marked 3), and for the probable EBL density (marked 2, see explanation in text). The c_0 curves are shown as solid lines. The c_1 and c_2 curves are shown as dashed and dotted lines respectively.

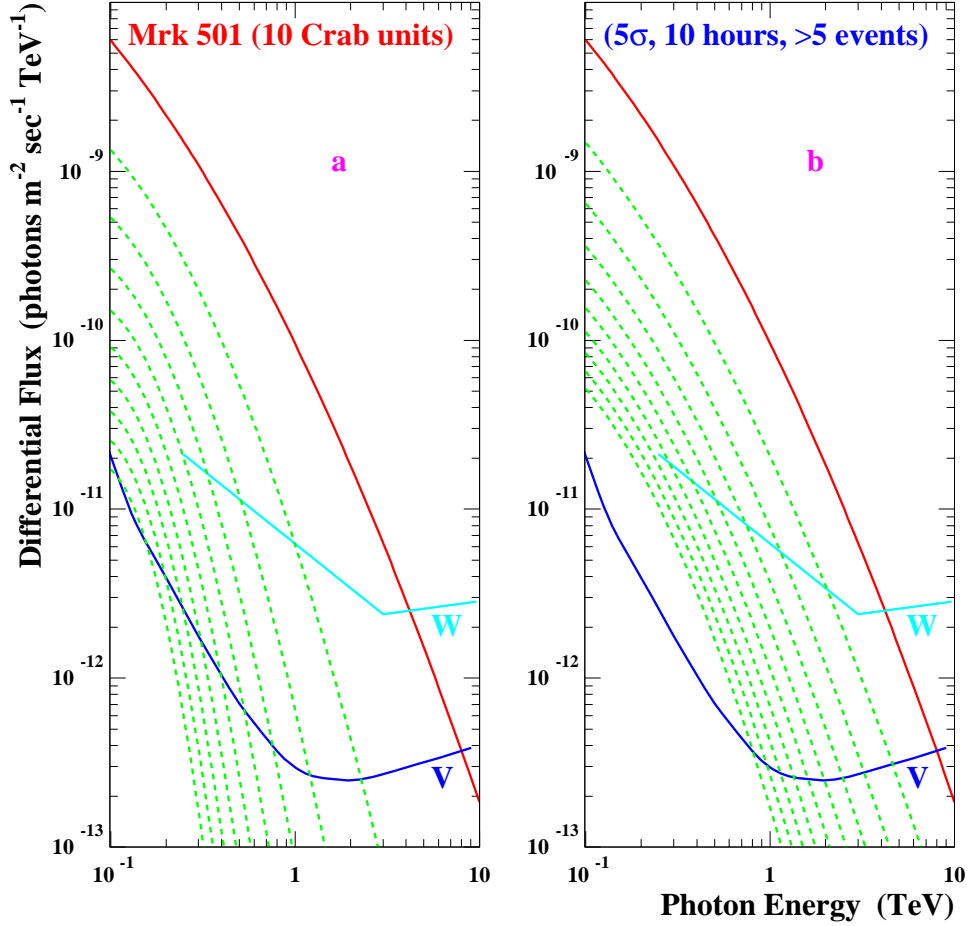


Fig. 9. The change of the observable spectrum of a hypothetical “Mrk 501-like” object during its highest activity if it is placed at higher redshifts. Figure “a” shows the maximum allowable EBL absorption effect. Figure “b” indicates the opposite limit. The sensitivities of Whipple and VERITAS are marked as “W” and “V” (see explanation in text). The solid line shows the Mrk 501 spectrum ($z = 0.03$) extrapolated into the 100 – 250 GeV region. The absolute flux of the blazar is 10 Crab units. The dashed lines correspond to the spectra of such AGN if observed at redshift $z = 0.06, 0.09, \dots, 0.3$.

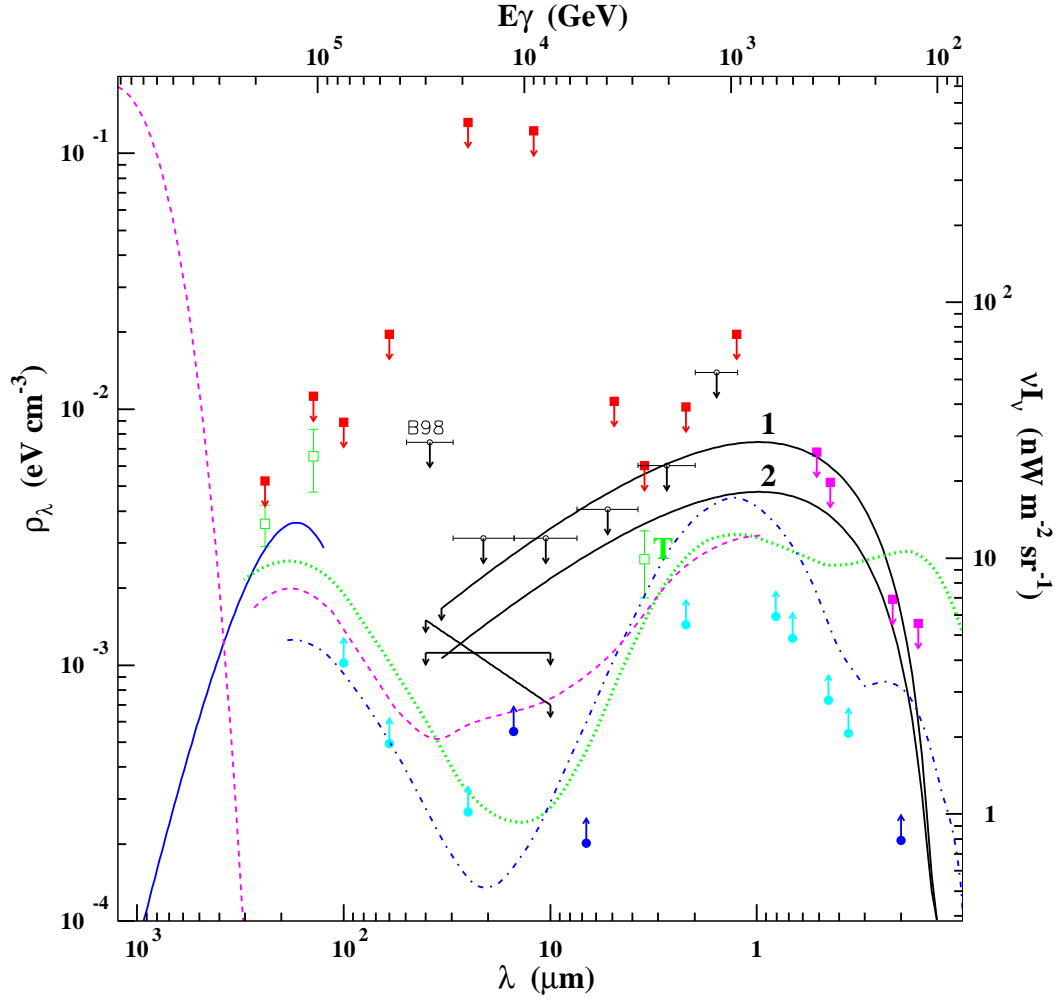


Fig. 10. The solid line marked “1” provides an upper limit in the range $\sim 1 - 30 \mu\text{m}$ on the SED EBL derived in this work. The range of the EBL SED between curves “1” and “2” is preferable if all curvature observed in the spectra of Mrk 501 and Mrk 421 is attributed to EBL absorption. Upper limits from the Mrk 501 TeV spectrum by Biller, et al. (28) normalized at the $3.5 \mu\text{m}$ *DIRBE* upper limit are shown as horizontal bars with arrows. “No cutoff” upper limits from Mrk 421 spectra are indicated in the range $10 - 40 \mu\text{m}$ by solid line segments with arrows (see explanation in text). Dotted line is LCDM (Salpeter) model by Primack et al. (14), and dot-dashed line is LCDM (Scalo) model from the same publication. Dashed line is “high” EBL model by Malkan & Stecker (25). Filled squares and circles indicate upper and low EBL limits respectively (see Fig. 1 for explanation).